Improving Real-Time Kinematic PPP with Instantaneous Cycle-Slip Correction

Simon Banville and Richard B. Langley, *University of New Brunswick, Canada*

BIOGRAPHY

Simon Banville is a Ph.D. candidate in the Department of Geodesy and Geomatics Engineering at the University of New Brunswick. He received a M.Sc. (Hons.) in 2007 from Laval University, Quebec, where he first got involved in precise point positioning.

Richard B. Langley is a professor in the Department of Geodesy and Geomatics Engineering at UNB, where he has been teaching and conducting research since 1981. He has a B.Sc. in applied physics from the University of Waterloo and a Ph.D. in experimental space science from York University, Toronto. Prof. Langley has been active in the development of GPS error models since the early 1980s and has been a contributing editor and columnist for GPS World magazine since its inception. He is a fellow of The Institute of Navigation (ION) and the Royal Institute of Navigation. He was a co-recipient of the ION Burka Award for 2003 and received the ION Johannes Kepler Award in 2007.

ABSTRACT

Nowadays, still few people use precise point positioning (PPP) to process GPS data from a moving receiver because the quality of the solution is extremely vulnerable to interruptions in signal tracking. A loss of lock on all GPS signals simultaneously implies that users may have to wait for several minutes (even hours in certain cases) before obtaining cm-level precision.

To avoid such a scenario, this paper proposes a method to instantaneously mitigate the impacts of signal interruptions (cycle slips). The approach is based on a time-differenced solution which allows estimating the size of cycle slips in a least-squares adjustment. Since cycle slips are integers by definition, a three-step method is proposed to increase the success rate of the integer-fixing procedure.

With GPS observations available at a one-second sampling interval, the proposed algorithm corrected 99% of cycle slips in the three data sets presented. The success rate decreases gradually as data gaps are introduced in the observations due to a temporal decorrelation of error sources. Other factors degrading the performance of the approach are also identified, providing a clear overview of the aspects to be improved.

INTRODUCTION

Over the last decade, precise point positioning (PPP) proved to be a powerful processing strategy. It vastly spread in several fields of applications such as atmospheric sciences, geodynamics, surveying in remote regions, processing of large networks, etc. On the other hand, the success of this technique in kinematic mode (with a moving receiver) is still muted due to a rather long convergence period required to obtain a centimeter-level of precision. Several efforts were mounted to overcome this limitation, which led to the recent possibility of fixing carrier-phase ambiguities to integers in PPP [*Laurichesse and Mercier, 2007; Collins, 2008; Ge et al., 2008; Mervart et al., 2008*], which is the key to reducing the convergence period.

Ambiguity resolution in PPP is still not a trivial task. Several error sources need to be carefully modeled in order to maintain their influence below an acceptable threshold. Hence, on-the-fly ambiguity resolution is not currently achievable, at least not with a high level of confidence. Furthermore, a moving receiver increases the risks of experiencing losses of lock on one or several satellites. In such instances, a new ambiguity resolution attempt needs to be performed. Since most ambiguity resolution approaches in PPP require averaging of the widelane ambiguities, this process is not achievable instantaneously and can lead to a temporary decrease in the overall performance of the system. Even cycle slips on single satellites can weaken the geometry and they have non-negligible impacts on the computed positions.

Current PPP software implementations seem to add large amounts of process noise to ambiguity variances when cycle slips are detected. This approach does not exploit the integer nature of cycle slips and can result in a degraded performance of PPP processing. This situation can easily be shown by artificially introducing cycle slips on all carrier-phase measurements simultaneously and

observing the impact on the coordinates' time series. As an example, Figure 1 compares the estimated height component of IGS station ALGO, as estimated from data collected on 10 April 2009, with cycle slips artificially introduced every 15 minutes on all satellites (more details regarding the processing strategy will be given in a subsequent section).

Two types of solution have been computed: one using a "conventional" PPP approach (i.e. by adding a large amount of process noise to the ambiguity variances when cycle slips are detected), and another one using the cycle-slip correction algorithm that will be described in this paper. Note that the "conventional" PPP approach presented offers similar results to those of well-established PPP software.

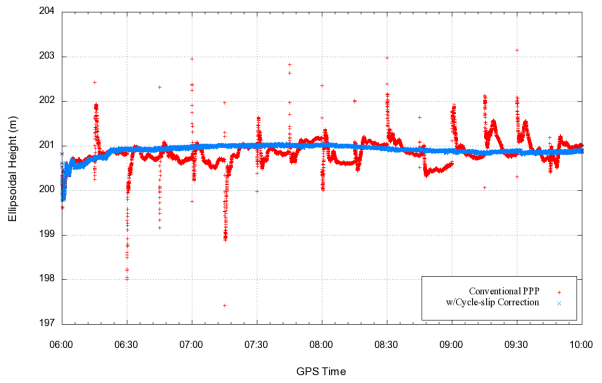

Figure 1 - Comparison of the estimated height obtained from a "conventional" PPP solution and from the cycle-slip correction algorithm for station ALGO on 10 April 2009.

Notice that, in the "conventional" PPP approach, a new convergence period is required every time cycle slips were introduced on all carrier-phase measurements simultaneously. This is typical of kinematic PPP solutions, since the filter must rely mainly on pseudorange measurements to estimate the coordinates and the receiver clock offset before the carrier-phase ambiguity parameters can regain a satisfactory precision. When applying the cycle-slip correction algorithm, cycle slips were properly repaired in all instances, which allowed obtaining a continuous convergence of the position.

Although several cycle-slip correction methods have been developed over the years, not all of them can be applied to the problem at hand. Polynomial fitting of carrier-phase observations [*Beutler et al., 1984*] or of linear combinations of observations [*Blewitt, 1990; Bisnath, 2000*] is certainly a widespread approach which has however limited applications in real-time processing. Moreover, filtering of the code-carrier divergence using a Kalman filter [*Bastos and Landau, 1988*] could fail to provide candidates that are precise enough to enable distinguishing certain pairings of ambiguities on L1 and L2.

An applicable approach is the one developed by *Kim and Langley* [2001], which estimates the size of cycle slips using a time-differenced (TD) solution. In this paper, we first review the principles underlying this approach, and then propose some modifications to account for the fact that the original method was based on relative positioning rather than on the use of a single receiver. The performance of this new implementation is assessed in challenging scenarios including continuous cycle slips on all carrier-phase measurements simultaneously and data gaps. Finally, shortcomings of the approach are exposed and discussed.

TIME-DIFFERENCED FUNCTIONAL MODEL

Time-differenced (TD) positioning utilizes variations in carrier-phase and code measurements over a certain time interval to estimate the change in receiver position and receiver clock offset during this period. In order to obtain an accurate estimate for those quantities, the variation of additional error sources must also be accounted for, which leads to the following functional model:

$$\delta\Phi_i = \delta\rho + c(\delta dT - \delta dt) - \delta I_i + \lambda_i \delta N_i + \varepsilon_{\delta\Phi_i} \quad (1)$$

$$\delta P_i = \delta\rho + c(\delta dT - \delta dt) + \delta I_i + \varepsilon_{\delta P_i} \quad (2)$$

where

i	identifies frequency-dependant terms
$\delta\Phi_i$	is the variation in accumulated delta range, obtained by differencing successive carrier-phase measurements (m)
δP_i	is the variation in pseudorange measurement between epochs (m)
$\delta\rho$	is the variation in instantaneous range between the phase center of the satellite and receiver antennas, including variations in tropospheric delay, earth tides, ocean loading and relativistic effects (m)
c	is the vacuum speed of light (m/s)
δdT	is the variation in the receiver clock offset (s)
δdt	is the variation in the satellite clock offset (s)
δI_i	is the variation in ionospheric delay (m)
λ_i	is the wavelength of the carrier (m)

δN_i is the variation of the carrier-phase ambiguity (i.e. the size of the cycle slip) (cy)

$\varepsilon_{\delta\Phi_i}, \varepsilon_{\delta P_i}$ are the measurement noise variations, including multipath (m)

Several studies focused on the temporal characteristics of the error sources affecting GPS observations (see e.g. *Olynik et al.* [*2002*]). Since most error sources are strongly correlated over a short period of time (e.g. a few seconds), their effects are greatly attenuated when forming the time-differenced signal combinations expressed by equations 1 and 2. For this purpose, the current study is based on the assumption that the sampling interval between measurements does not exceed a few seconds, which is a reasonable scenario in numerous kinematic applications. For instance, a vehicle passing under an overpass or through a short tunnel will experience such a signal blockage.

Even if the contribution of many error sources is greatly mitigated, one inevitably has to properly account for the variation in satellite positions and geometry change between epochs. In this research, this process is done following the methodology proposed by *Van Graas and Soloviev* [2004]. This formulation allows using the same coordinates' design matrix for both PPP and time-differenced solutions.

Furthermore, to achieve the level of accuracy required in the algorithm described herein, the variation in satellite clock errors and tropospheric delay should at least be accounted for. Unfortunately, the variation in ionospheric delay is complex to model when cycle slips are present in the carrier-phase measurements. This issue will be discussed in more detail later.

As mentioned previously, the quantities of interest in equations 1 and 2 are usually the change in receiver position (contained in $\delta\rho$), and the variation of the receiver clock offset (δdT). In this type of processing, cycle slips (δN_i) are usually considered as nuisance parameters, and carrier-phase measurements affected by such slips are simply disregarded for those particular epochs. In this research, cycle-slip parameters are the core of the algorithm and are included in the functional model.

One might have noticed that equations 1 and 2 did not include any terms accounting for instrumental delays. Since the time-span between two successive epochs is relatively short, the variation in instrumental biases can be safely neglected. This means that cycle slips preserve their integer nature and ambiguity resolution techniques can be applied to recover the size of those slips. This is the principle underlying the algorithm presented herein and further details on the ambiguity fixing process will be outlined in the next section.

CYCLE-SLIP CORRECTION

The functional model described previously can be expressed in a linearized form as:

$$\boldsymbol{y} = \boldsymbol{A}\boldsymbol{x} + \boldsymbol{B}\boldsymbol{n} + \boldsymbol{e}, \quad \boldsymbol{x} \in \mathbb{R}^4, \boldsymbol{n} \in \mathbb{Z}^n$$
$$Cov[\boldsymbol{y}] = \boldsymbol{Q} \tag{3}$$

where

$\boldsymbol{y}$ is the vector of differences between the time-differenced observations (see equations 1 and 2) and their computed values

$\boldsymbol{x}$ is the vector of unknown geometric parameters such as receiver position and receiver clock offset variations

$\boldsymbol{n}$ is the *n*-dimension vector of cycle-slip parameters

$\boldsymbol{e}$ is the vector of unmodelled errors associated with each observation

A, **B** are the design matrices associated with the unknown geometric parameters and cycle-slip parameters respectively

It is recommended that a cycle-slip parameter be added for a given carrier-phase measurement solely when a cycle slip has been detected. For this purpose, cycle-slip detection methods such as the one described by *Blewitt* [1990] or *Bisnath* [2000] can be used. Introducing extra cycle-slip parameters reduces the geometric strength of the solution and increases the computational burden.

As a first step, the system can be solved by disregarding the integer constraint on cycle-slip parameters. Then, float values for the cycle-slip parameters ($\hat{\boldsymbol{n}}$) and their covariance matrix ($\boldsymbol{Q}_{\hat{\boldsymbol{n}}}$) can be extracted from the system for the ambiguity fixing procedure. In theory, fixing the cycle-slip candidates $\hat{\boldsymbol{n}}$ to integers could be performed using any ambiguity resolution method developed for this purpose [*Kim and Langley, 2000*]. On the other hand, since instantaneous cycle-slip correction is expected, the method chosen must allow quickly determining the correct set of integers.

When carrier-phase measurements on at least 4 satellites are free of cycle slips, fixing cycle-slip parameters to integers is, most of the time, a trivial task. Indeed, the precision of the estimated parameters is often within a fraction of a cycle due to the inherent precision of carrier-phase observations.

A critical scenario happens when cycle slips have been detected on all carrier-phase measurements at a given epoch. The ambiguity search space is then defined by the

noisy pseudorange measurements and, even when using the LAMBDA method [*Teunissen, 1994*], cycle slips on L1 and L2 cannot necessarily be fixed with a satisfactory success rate (refer to section "Processing Results" for more details). This can be explained by the fact that the hyper-ellipsoid defining the ambiguity search space is often not centered near the correct set of integers. A means to reduce this bias consists of using Doppler measurements (if available) or the narrowlane linear combination of pseudoranges since the noise level associated with those measurements is lower. Nevertheless, this improvement was found not to be a viable alternative to obtain a high ambiguity-fixing success rate.

The approach adopted in this research is inspired by the work of *Colombo et al.* [1999]. First, the widelane (WL) ambiguities (cycle slips) are fixed with the help of the LAMBDA method. Since the wavelength of this linear combination is much larger (≈86 cm as opposed to ≈19 cm for the L1 carrier), it is less sensitive to a bias in the initial solution.

The next step uses the time-differenced geometry-free (GF) ambiguities with the introduction of the previously fixed widelane ambiguities ($\delta\breve{N}_{WL}$) to determine the size of the cycle slips on L1:

$$\delta\breve{N}_1 = round\left[\frac{\delta\hat{N}_{GF} - \lambda_2\delta\breve{N}_{WL}}{\lambda_1 - \lambda_2}\right] \quad (4)$$

with

$$\delta\hat{N}_{GF} = \lambda_1\delta\hat{N}_1 - \lambda_2\delta\hat{N}_2 \quad (5)$$

The time-differenced geometry-free combination is affected mainly by the variation in ionospheric delay between the two epochs, but this variation is often negligible if the sampling interval is short enough. By first introducing the fixed widelane ambiguities, the resulting L1 ambiguities have a wavelength of 5.4 cm. This means that the contribution of unmodeled errors should not exceed about 1.4 cm in order to fix reliably the L1 ambiguities to integers. As will be shown in the "Processing Results" section, this condition is satisfied in most cases for a short time interval. However, residual ionospheric errors and multipath in low-elevation-angle satellites can sometimes exceed this tight threshold.

Since the quality of the solution in kinematic positioning depends largely on the geometry of satellites, uncorrected cycle slips will inevitably degrade the precision of the estimated parameters. Thus, to obtain the most precise solution, it is recommended to perform an extra step when only a subset of cycle slips ($\boldsymbol{n_a}$) has been corrected using equation 4. Since cycle-slip parameters are strongly correlated with each other, one could make use of the "bootstrapping" technique [*Blewitt, 1989*] to increase the precision of the remaining unfixed cycle slips ($\boldsymbol{n_b}$):

$$\hat{\boldsymbol{n}}_{\boldsymbol{b}}' = \hat{\boldsymbol{n}}_{\boldsymbol{b}} - \boldsymbol{Q}_{\hat{n}_b\hat{n}_a}\boldsymbol{Q}_{\hat{n}_a}^{-1}(\hat{\boldsymbol{n}}_{\boldsymbol{a}} - \breve{\boldsymbol{n}}_{\boldsymbol{a}}) \quad (6)$$

$$\boldsymbol{Q}_{\hat{n}_b'} = \boldsymbol{Q}_{\hat{n}_b} - \boldsymbol{Q}_{\hat{n}_b\hat{n}_a}\boldsymbol{Q}_{\hat{n}_a}^{-1}\boldsymbol{Q}_{\hat{n}_a\hat{n}_b} \quad (7)$$

Another attempt at fixing the components of $\hat{\boldsymbol{n}}_{\boldsymbol{b}}'$ to integers can then be performed. The whole process is summarized in Figure 2 and the corresponding equations are given between parentheses.

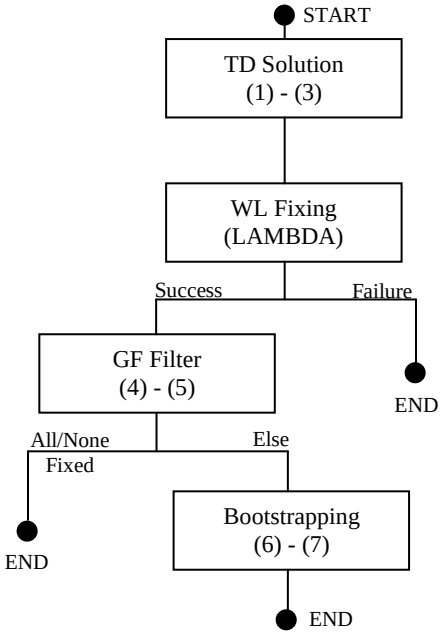

Figure 2 - Proposed cycle-slip correction algorithm

The size of the cycle slips on both L1 and L2 being determined, the effect of the slips can be removed by modifying the predicted values of the ambiguity parameters in the PPP filter. By doing so, the covariance matrix of the predicted ambiguities remains unchanged, which provides continuous coordinate time series. Validation of the chosen integer cycle-slip candidates can be done in the PPP filter by performing a data snooping test [*Baarda, 1968*].

PROCESSING RESULTS

The usefulness of the approach described in this paper would be significant provided that on-the-fly cycle-slip correction could be performed reliably under different tracking conditions. The critical factors to consider are as follows:

1. Simultaneous cycle slips on all carrier-phase measurements

2. Data gaps (resulting in a temporal decorrelation of error sources)
3. Multipath and noise

In order to evaluate the performance of our approach under those conditions, virtual cycle slips were introduced on all carrier-phase measurements at every epoch contained in the RINEX files processed (i.e. no real cycle slips were introduced in the data but the software was modified to constantly assume cycle slips). In other words, carrier-phase measurements cannot contribute to the PPP solution unless cycle slips are adequately corrected.

All original RINEX files used in the following tests contained observations at a 1-second sampling interval. The impact of data gaps was analyzed by decimating the files to produce 10, 20 and 30-second sampling intervals.

Finally, the effects of multipath and noise are assessed by using data collected under different receiver dynamics. First, observations from a static IGS station is processed using an epoch-by-epoch approach making no assumptions on the receiver dynamics. Then, kinematic trajectories of a boat and a car are computed using the same approach.

In all scenarios, products from the International GNSS Service (IGS) available in real time were used such as the predicted part of ultra-rapid satellite orbits and Earth orientation parameters, as well as real-time satellite clock corrections [*Caissy, 2009*]. The tropospheric delay was obtained using pressure values and mapping function coefficients from the forecast Vienna Mapping Function 1 [*Boehm et al., 2009*], computed following *Kouba* [2008]. No residual tropospheric zenith delay was estimated in the filter, which has no impact on the results presented hereafter.

Since the key to instantaneous cycle-slip correction is an efficient ambiguity-fixing algorithm, the performance of three approaches is compared:

1. Fixing ambiguities on both L1 and L2 using the LAMBDA method; i.e., resolving all ambiguities as a set.
2. Fixing the widelane (WL) and geometry-free (GF) ambiguities as described previously.
3. Using the WL/GF method and performing an additional bootstrapping (BS) step (equations 6 and 7).

Test #1: Static Receiver

The first test performed uses data from IGS station ALGO, from 6:00 to 10:00 GPST, on 10 April 2009. Since the antenna is not moving, multipath conditions are slowly changing which constitutes a helpful factor for instantaneous cycle-slip correction. This test is thus a "best-case" scenario for the assessment of our algorithm.

Table 1 shows the cycle-slip correction success rate for different scenarios. The success rate is defined as the ratio of the number of corrected cycle slips over the total number of cycle slips introduced in the data sets (i.e. on all carrier-phase measurements at each epoch). For example, when attempting to fix ambiguities directly on L1 and L2 at a 1-second sampling interval, 233270 cycle slips were corrected out of the 242546 that were present in the data set which gives a 96.2% success rate.

Table 1 - Cycle-slip correction success rate for station ALGO

Sampling (sec)	**1**	**10**	**20**	**30**
# CS	242546	24236	12110	8064
L1&L2	233270 (96.2%)	23740 (98.0%)	11694 (96.6%)	7696 (95.4%)
WL/GF	242068 (99.8%)	24166 (99.7%)	12048 (99.5%)	7962 (98.7%)
WL/GF/BS	242068 (99.8%)	24166 (99.7%)	12058 (99.6%)	7980 (99.0%)

Since the quality of the positioning solution is increased every time a single cycle slip is corrected, the improvement of the WL/GF approach over the L1&L2 approach is non negligible. However, performing the bootstrapping step did not improve the results for a sampling interval of 1 and 10 seconds. This is due to the fact that, in all instances, the widelane ambiguities could not be fixed to integers. Referring to Figure 2, one can notice that failure to fix the widelane ambiguities puts an end to the cycle-slip correction algorithm. Hence, bootstrapping will obviously not improve the solution in such a case.

It is also logical to observe a decreasing success rate when the sampling interval increases. In such an occurrence, the temporal correlation of error sources diminishes resulting in unmodeled errors in the functional model. An exception occurs for the L1&L2 method for which the success rate is higher at intervals of 10 and 20 seconds than at a 1-second sampling interval. This result can be explained by the fact that cycle slips could not be corrected for several consecutive 1-second epochs, which affected considerably the corresponding success rate. When decimating the file, the impact of this phenomenon has been greatly attenuated.

Although data gaps of 30 seconds were considered here, it is important to stress that ionospheric delay variations during such an interval could become important during periods of moderate to high ionospheric activity. This

could lead to cycle slips being fixed to the wrong integers if an appropriate means of validating the candidates is not properly implemented. It is then recommended to use the algorithm parsimoniously if rapid ionospheric delay fluctuations are anticipated.

Test #2: Boat Trajectory

As a second test, the performance of the algorithm is assessed using observations collected using a C-Nav2050M GPS receiver on board a boat surveying a region of the Bay of Fundy in eastern Canada. The data used covers a period from 16:00 to 18:30 GPST on 11 May 2009. The boat was moving at a speed ranging approximately between 2 and 9 knots throughout this period. The estimated trajectory and height profile are depicted in Figures 3 and 4. The cycle-slip correction success rate is included in Table 2.

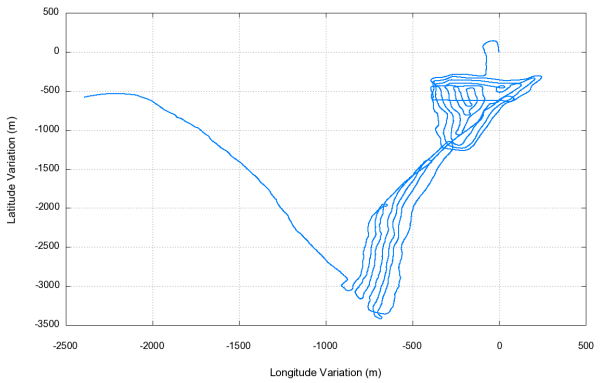

Figure 3 - Horizontal relative displacement of the boat

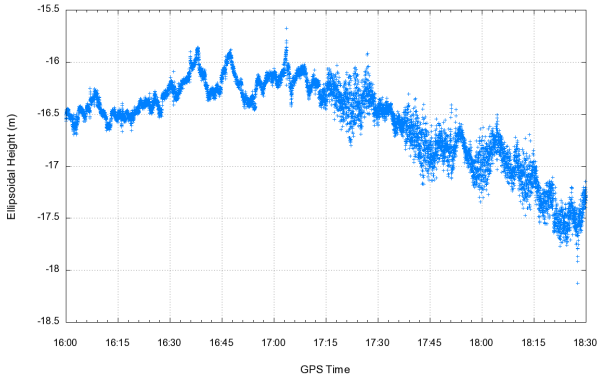

Figure 4 - Ellipsoidal height profile of the boat's trajectory

Again, all cycle-slip correction methods performed relatively well for a 1-second sampling interval. Almost all cycle slips were corrected when using the third approach, which demonstrates the advantages of performing the bootstrapping step. However, the success rate decreases dramatically for a 10-second interval in the case of the L1&L2 method. The same phenomenon is observed for the two other approaches when data gaps of 20 seconds or more are present in the observation time series.

The explanation for this sudden drop in the performance of the algorithm can be deduced by observing the trajectory of the boat in Figure 3. Since GPS signals have a right-hand circular polarization, a rotation of the transmitting or receiving antenna leads to a change in the measured phase [*Wu et al., 1993*]. In the GPS literature, this phenomenon is called phase wind-up or phase wrap-up. Modeling of the satellite component of the wind-up effect is a well-known procedure that must be accounted for in the PPP functional model and in long-baseline differential processing. On the other hand, the receiver component is often ignored since it is quite challenging to model due to the absence of attitude information. Neglecting this correction has a known impact on differential positioning [*Kim et al., 2006*], but its effect on PPP has, to the author's knowledge, not been studied.

Table 2 - Cycle-slip correction success rate for the boat trajectory

Sampling (sec)	1	10	20	30
# CS	160288	16000	7978	5310
L1&L2	156300 (97.5%)	2148 (13.4%)	38 (0.5%)	18 (0.3%)
WL/GF	159227 (99.3%)	15486 (96.8%)	1288 (16.1%)	350 (6.6%)
WL/GF/BS	160268 (100%)	15822 (98.9%)	1350 (16.9%)	378 (7.1%)

If the antenna rotates around its boresight, the wind-up effect should be the same on all carrier-phase measurements and thus absorbed by the receiver clock. In the TD functional model however, the pseudorange measurements, which are not affected by this effect, contribute to the estimation of the receiver clock offset variation which creates an incompatibility in the model. When cycle slips occur on all carrier phases, the receiver clock is estimated using solely the pseudoranges and the wind-up effect is absorbed by the cycle-slip parameters.

Figure 5 shows the variation of the geometry-free combination for PRN15. A quadratic fit has been removed from the time series to account for the approximate variation of ionospheric delay caused by the change in satellite elevation angle. The remaining signal in the data is the receiver component of the wind-up effect. This affirmation was confirmed by observing a similar signal on all satellites and by correlating the fluctuations with the changes in direction of the boat. This information is also included in Figure 5 by means of the number of rotations of the antenna (a negative value denotes a counter-clockwise rotation of the antenna)

computed from the changes in receiver horizontal coordinates. Note that part of the accumulated wind-up has been absorbed by the polynomial fitting.

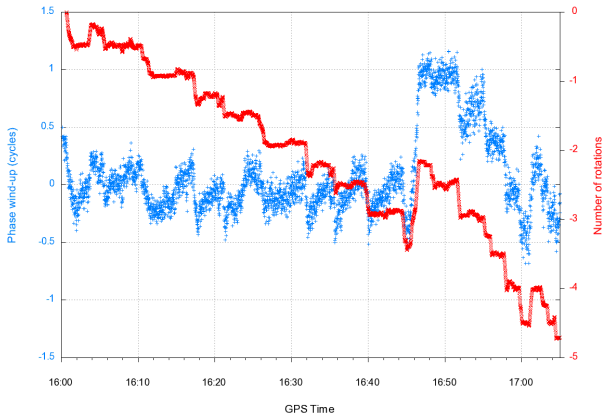

Figure 5 - Receiver component of the phase-wind-up effect as shown on PRN15

Since the boat was performing surveying operations, the antenna rotated regularly, resulting in a prominent wind-up effect with a short correlation time. The consequence on the L1&L2 cycle-slip correction success rate is obvious. Since the widelane ambiguities are not affected by the wind-up effect, the second and third methods were not affected as drastically. Those methods still ended up failing due to the geometry-free ambiguities which are also sensitive to phase wind-up.

Test #3: Car Trajectory

The last data set examined in this paper is a short car trajectory (shown on Figures 6 and 7) on 10 April 2008, lasting approximately 30 minutes. The GPS data was collected using a NovAtel OEMV-3 receiver in the streets of Fredericton, New Brunswick, Canada. Since the real-time satellite clock corrections were not yet available at this time, the predicted values accompanying the ultra-rapid orbit product were used.

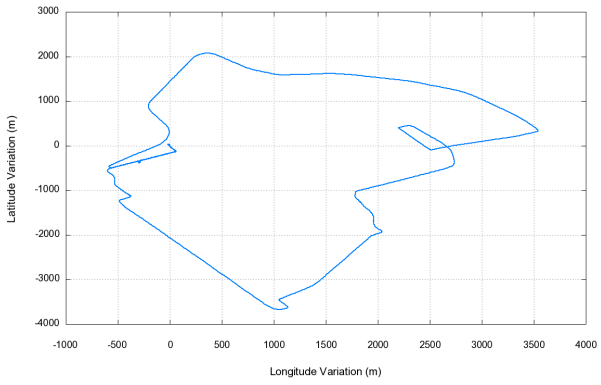

Figure 6 - Horizontal relative displacement of the car

The car went under several dense tree canopies, resulting in numerous losses of lock on the GPS signals. Figure 8 gives an overview of the number of satellites tracked at each epoch. As one can see from Table 3, the rapidly changing geometry clearly had an impact on the results.

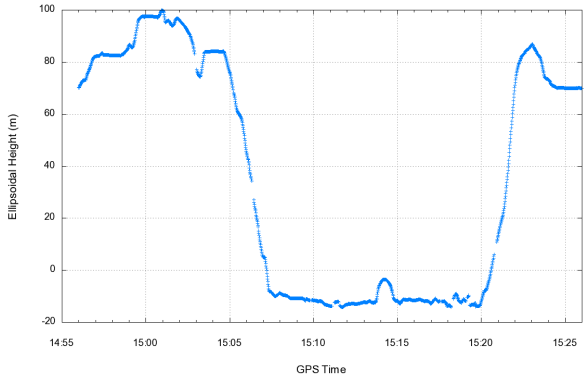

Figure 7 - Ellipsoidal height profile of the car's trajectory

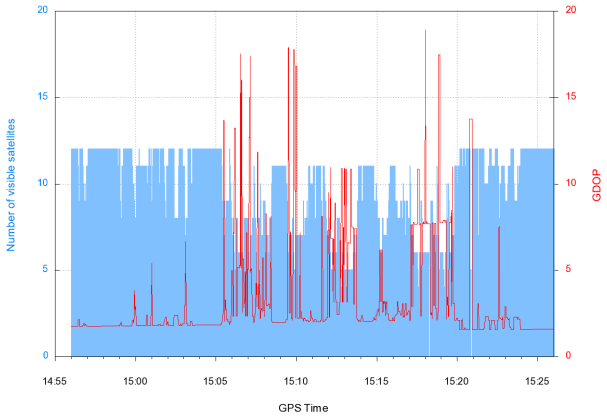

Figure 8 - Number of visible satellites

Table 3 - Cycle-slip correction success rate for the car trajectory

Sampling (sec)	1	10	20	30
# CS	32966	3042	1550	920
L1&L2	32150 (97.5%)	818 (26.9%)	160 (10.3%)	98 (10.7%)
WL/GF	32720 (99.3%)	1818 (59.8%)	472 (30.5%)	276 (30.0%)
WL/GF/BS	32778 (99.4%)	1876 (61.7%)	502 (32.4%)	300 (32.6%)

When all epochs were preserved in the original data set, the success rate of the second and third approaches again provided a cycle-slip correction success rate above 99%. However, the quick decorrelation of the multipath effect affecting pseudorange measurements and the frequent weak geometric strength of the time-differenced solution caused a rapid decrease of the performance of all methods

when data gaps were introduced. The contribution of unmodeled phase wind-up should again be pointed out, especially when the vehicle made sharp turns.

Naturally, this test represented a really challenging scenario. Although multipath conditions can vary rather suddenly for a moving vehicle, cycle slips usually do not occur on all carrier-phase measurements at all epochs. One could then make use of the phase measurements unaffected by cycle slips to constrain the cycle-slip candidates search space and obtain better results.

SUMMARY AND CONCLUSIONS

Since it is currently a complex task to fix carrier-phase ambiguities on the fly in PPP, a means of effectively accounting for cycle slips is crucial. Failure to do so may seriously degrade the quality of the solution when cycle slips contaminate several carrier-phase measurements simultaneously. In this paper, we presented a method for correcting cycle slips instantaneously: i.e., within a single epoch. It is based on the concept of a time-differenced solution in which the size of cycle slips is estimated as a part of a least-squares adjustment.

With a sampling interval of one second, cycle slips could be corrected with a success rate of approximately 99% for the three data sets tested. These results are a promising outcome for kinematic PPP which still lacks the reliability and consistency of differential RTK positioning. Note that the approach could also be applied to improve static PPP solutions covering a short time-span.

The performance of the algorithm decreases when data gaps occur due to the temporal decorrelation of error sources. The tests carried out also allowed us to establish that the method is particularly sensitive to unmodeled changes in ionospheric delay variations, to the receiver component of the phase wind-up effect, to quick variations of the multipath characteristics, and to the weak geometric strength of the time-differenced solution. Work has already been initiated at UNB to account for the ionospheric effects and results should be presented to the GNSS community in a near future.

ACKNOWLEDGMENTS

Special thanks are due to the Natural Sciences and Engineering Research Council of Canada (NSERC), the Geomatics for Informed Decisions (GEOIDE) Network of Centres of Excellence and the School of Graduate Studies at the University of New Brunswick for their financial support.

The GPS data for the boat trajectory was kindly provided by the Ocean Mapping Group of the Department of Geodesy and Geomatics Engineering at the University of New Brunswick. We would also like to acknowledge Hyunho Rho, Ph.D. candidate in the same department, for sharing the car trajectory data set.

REFERENCES

Baarda, W. (1968). *A Testing Procedure for Use in Geodetic Networks*. Publications on Geodesy, New Series, Vol. 2, No. 5, Netherlands Geodetic Commission.

Bastos, L. and H. Landau (1988). "Fixing Cycle Slips in Dual-frequency Kinematic GPS-applications Using Kalman Filtering." *Manuscripta Geodaetica*, Vol. 13, No. 4, 1988, pp. 249-256.

Beutler, G., D.A. Davidson, R.B. Langley, R. Santerre, P. Vanicek and D.E. Wells (1984). *Some Theoretical and Practical Aspects of Geodetic Positioning Using Carrier Phase Difference Observations of GPS Satellites*. Technical Report No. 109, University of New Brunswick, Canada, 79 pages.

Bisnath, S.B. (2000). "Efficient Automated Cycle-slip Correction of Dual-frequency Kinematic GPS Data." *Proceedings of ION GPS 2000*, Salt Lake City, Utah, 19-22 September, pp. 145-154.

Blewitt, G. (1989). "Carrier-phase Ambiguity Resolution for the Global Positioning System Applied to Geodetic Baselines up to 2000 km." *Journal of Geophysical Research*, Vol. 94, No. B8, pp. 10187-10203.

Blewitt, G. (1990). "An Automatic Editing Algorithm for GPS Data." *Geophysical Research Letters*, Vol. 17, No. 3, pp. 199-202.

Boehm, J., J. Kouba, and H. Schuh (2009). "Forecast Vienna Mapping Functions 1 for Real-time Analysis of Space Geodetic Observations." *Journal of Geodesy*, Vol. 83, No. 5, pp. 397-401.

Caissy, M. (2009). "Status of IGS Real Time Pilot Project". IGSMAIL-5927, April 3 2009.
http://igscb.jpl.nasa.gov/mail/igsmail/2009/

Collins, P. (2008). "Isolating and Estimating Undifferenced GPS Integer Ambiguities." *Proceedings of ION NTM 2008*, San Diego, Calif., 28-30 January, pp. 720-732.

Colombo, O.L., M. Hernández-Pajares, J.M. Juan, J. Sanz, and J. Talaya (1999). "Resolving Carrier-Phase Ambiguities On The Fly, at More Than 100 km from Nearest Reference Site, with the Help of Ionospheric Tomography." *Proceedings of ION GPS 1999*, September 14-17, Nashville, TN, pp. 1635-1642.

Ge, M., G. Gendt, M. Rothacher, C. Shi and J. Liu (2008). "Resolution of GPS Carrier-phase Ambiguities in Precise Point Positioning (PPP) with Daily Observations." *Journal of Geodesy*, Vol. 82, No. 7, pp. 389-399.

Kim, D. and R.B. Langley (2000). "GPS Ambiguity Resolution and Validation: Methodologies, Trends and Issues." *Proceedings of the 7th GNSS Workshop – International Symposium on GPS/GNSS*, Seoul, Korea, November 30 – December 2, pp. 213–221.

Kim, D. and R.B. Langley (2001). "Instantaneous Real-time Cycle-slip Correction of Dual-frequency GPS Data." *Proceedings of the International Symposium on Kinematic Systems in Geodesy, Geomatics and Navigation*, Banff, Alberta, Canada, 5-8 June, pp. 255-264.

Kim, D., L. Serrano, and R.B. Langley (2006). "Phase Wind-up Analysis: Assessing Real-time Kinematic Performance." *GPS World*, Vol. 17, No. 9, September, pp. 58-64.

Kouba, J. (2008) "Implementation and Testing of the Gridded Vienna Mapping Function 1 (VMF1)." *Journal of Geodesy*, Vol. 82, No. 4-5, pp. 193-205.

Laurichesse, D. and F. Mercier (2007). "Integer Ambiguity Resolution on Undifferenced GPS Phase Measurements and its Application to PPP." *Proceedings of ION GNSS 2007*, Fort Worth, Texas, 25-28 September, pp. 839-848.

Mervart, L, Z. Lukes, C. Rocken, and T. Iwabuchi (2008). "Precise Point Positioning with Ambiguity Resolution in Real-Time." *Proceedings of ION GNSS 2008*, September 16-19, Savannah, Georgia, pp. 397-405.

Olynik, M., M.G. Petovello, M.E. Cannon, and G. Lachapelle (2002). "Temporal Impact of Selected GPS Errors on Point Positioning." *GPS Solutions*, Vol. 6, No. 1-2, pp. 47-57.

Teunissen, P.J.G. (1994). "A New Method for Fast Carrier Phase Ambiguity Estimation." *Proceedings IEEE Position, Location and Navigation Symposium PLANS'94*, Las Vegas, NV, April 11-15, pp. 562-573.

Van Graas, F. and A. Soloviev (2004). "Precise Velocity Estimation Using a Stand-Alone GPS Receiver." *Navigation: Journal of the Institute of Navigation*, Vol. 51, No. 4, pp. 283-292.

Wu, J., S. Wu, G. Hajj, W. Bertiger, and S. Lichten (1993). "Effects of Antenna Orientation on GPS Carrier Phase." *Manuscripta Geodaetica*, Vol. 18, No. 2, pp. 91–98.